Electronic Supplementary Information

Optimal d-band-Induced Cu_3N as Cocatalyst on Metal Sulfide for Boosting Photocatalytic Hydrogen Evolution

Qing Guo,[a,b] Fei Liang,[c] Zongzhao Sun,[a] Yang Wang,[d] Xubing Li,[d] Shuguang Xia,[d] Z. Conrad Zhang,[b] Limin Huang*,[a] and Li-Zhu Wu[d]

[a]*Department of Chemistry, Southern University of Science and Technology, Shenzhen, 518055, China*

[b]*State Key Laboratory of Catalysis, Dalian Institute of Chemical Physics, Chinese Academy of Sciences, Dalian 116023, China*

[c]*State Key Laboratory of Crystal Materials and Institute of Crystal Materials, Shandong University, Jinan 250100, China*

[d]*Key Laboratory of Photochemical Conversion and Optoelectronic Materials, Technical Institute of Physics and Chemistry, Chinese Academy of Sciences, Beijing 100190, China*

*To whom correspondence should be addressed.

E-mail: huanglm@sustech.edu.cn.

Table of Contents

1. Synthesis of Cu_3N NCs: Cubic phase Cu_3N nanocrystals were synthesized by reported methods.[1] Briefly, 60 mg $Cu(NO_3)_2 \cdot 2.5H_2O$ was dissolved in 5 mL oleylamine and 5 mL 1-octadecene. The solution was degassed under vacuum for 30 min. Then the flask was filled with highly pure argon (Ar) and heated at 150 ℃ for 3 h by heating mantle under magnetic stirring, in which the color of the solution changed from blue to green, and finally to yellow. After that, the solution was heated to 250 ℃ and kept at this temperature for 30 min. Subsequently, the heating mantle was removed and the flask was cooled down. The product was collected by centrifugation (12000 rpm, 10 min), washed with ethanol several times and finally dried at 60 ℃ under vacuum.

2. Synthesis of Cu_2O: Cu_2O was synthesized according to previous methods.[2] A mixture of $Cu(NO_3)_2 \cdot 2.5H_2O$ (1.0 g) and octadecylamine (ODA, 8.6 g) was placed in a flask and degassed under vacuum for 30 min. Then the flask was filled with Ar and heated at 240 ℃ for 10 min by heating mantle under magnetic stirring. Subsequently, heating mantle was removed and the flask was cooled down. The product was washed with ethanol several times and finally dried at 60 ℃ under vacuum.

3. Synthesis of Cu_2S: Cu_2S was prepared by reported methods.[3] Firstly, $Cu(NO_3)_2 \cdot 2.5H_2O$ (232 mg) was dissolved in deionized water (20 mL) to form a clear blue solution. Then, CH_3COONa (82 mg) and CH_3COOH (600 μL) were added into the above blue solution. After stirring for 15 min, it was transferred into a Teflon-lined autoclave and dodecanethiol (3 mL) was introduced. The solution was heated at 200 ℃ for 6 h. After cooling to room temperature, the product was collected by centrifugation (6000 rpm, 5 min) and washed with ethanol for several times. Finally, the product was dried at 60 ℃ for further use.

4. Synthesis of Cu_3P: Cu_3P was prepared according to literature methods.[4] In briefly, 1.16 g $Cu(NO_3)_2 \cdot 2.5H_2O$ was dissolved in 100 mL deionized water to form a clear solution. NaOH aqueous solution (0.25 mol/L, 20 mL) was introduced under magnetic stirring. After stirring for 2 h, precipitates of $Cu(OH)_2$ were collected by centrifugation and dried under vacuum. Then, the obtained $Cu(OH)_2$ (250 mg) was mixed with NaH_2PO_2 (2.5 g) and calcined at 300 ℃ for 1 h with a heating rate of 2.0 ℃ min^{-1} under Ar atmosphere. After that, the samples were collected and washed with water and ethanol for further applications.

5. Synthesis of CdS/Cu_3N: firstly, $Cd(CH_3COO)_2$ (368 mg) and thiourea (420 mg) were dissolved in deionized water (30 mL) to form a clear solution.[5] Then, 3.0 mg Cu_3N was dispersed into the solution through ultrasonication. After that, the solution was transferred into a Teflon-lined autoclave and kept at 180 ℃ for 12 h. The product was collected by centrifugation (8000 rpm, 5 min) and washed with water and ethanol several times. Finally, the product was dried at 60 ℃ for further characterizations and uses. The dosages of added Cu_3N were 0, 1.0, 2.0, 3.0, 5.0 and 9.0 mg, and the resulting mass ratios of Cu_3N to CdS were 0, 0.8, 1.3, 2.0, 3.1 and 3.9 wt%, respectively.

For the synthesis of CdS/Cu_2O, CdS/Cu_2S and CdS/Cu_3P, 3.0 mg Cu_2O, Cu_2S and Cu_3P were introduced respectively, instead of Cu_3N, and other procedures were similar to above.

6. Photocatalytic hydrogen production: the solar H_2 generation reaction was conducted in a closed glass reaction system (CEL-SPH2N, CEAULIGHT, Beijing). First of all, 10.0 mg photocatalyst CdS/Cu_3N was dispersed in 40.0 mL ascorbic acid (AA) aqueous solution (0.1 mol/L, pH = 5.0). Then, the air in reactor was evacuated using a vacuum pump for 15 min. After that, the reactor was irradiated by a 300 W Xe lamp with a cut-off filter of 400 nm. The generated molecular H_2 in the reactor system was measured using an online gas chromatograph system (*Shimadzu* GC2014CAFC/APC) equipped with a thermal conductivity detector and a 5 Å molecular sieves GC column. Ar was used as a carrier gas. Error bars on H_2 were calculated from at least three independent experiments. For the wavelength-dependent activities were measured using a bandpass filter of 420 nm, 450 nm, 500 nm, and 600 nm, respectively, instead of cut-off filter of 400 nm and other procedures were similar to above.

7. The measurement of apparent quantum yield (AQY): Briefly, 2.5 mL ascorbic acid (AA) aqueous solution (1.0 mol/L, pH = 5.0) containing 0.5 mg photocatalyst CdS/Cu_3N was placed in a sealed quartz cuvette with 1-cm path length. Then, the system was irradiated under 450 nm LEDs (100 mW · cm^{-2}) with a fixed irradiation area of 1.57 cm^2. The evolved H_2 gas during 2.0 h was analyzed by GC. As a result, the number of absorbed photons could be calculated as the following equation:

$$N_{photon} = \frac{t(s) \times P(W \cdot cm^{-2}) \times S(cm^2) \times \lambda(m)}{h(J \cdot s) \times c(m \cdot s^{-1})}$$

$$= \frac{2 \times 3600(s) \times 100 \times 10^{-3}(W \cdot cm^{-2}) \times 1.57(cm^2) \times 450 \times 10^{-9}(m)}{6.626 \times 10^{-34}(J \cdot s) \times 3 \times 10^{8}(m \cdot s^{-1})}$$

$$= 2.56 \times 10^{21}$$

So, the apparent quantum yield (AQY) of photocatalytic H_2 evolution was calculated as the following equation:

$$AQY = \frac{2n(H_2) \times 6.02 \times 10^{23}}{N_{photon}} \times 100\%$$

For the CdS/Cu_3N system, about 82.78 μmol of H_2 was produced in 2.0 h. Herein, the AQY can be calculated as follows:

$$AQY = \frac{2 \times 82.78 \times 10^{-6}(\text{mol}) \times 6.02 \times 10^{23}/mol}{2.56 \times 10^{21}} \times 100\%$$

$$= 3.9\%$$

8. Long-time photocatalytic H_2 evolution: firstly, 100.0 mg CdS/Cu_3N was dispersed in 50.0 mL AA aqueous solution (1.0 mol/L, pH = 5.0). The air in reactor was then evacuated using a vacuum pump for 15 min. The photocatalytic experiment was carried out under the irradiation of Xe lamp with a cut-off filter of 400 nm (300 W). The produced H_2 was detected every 0.5 h by an online gas chromatograph (*Shimadzu* GC2014CAFC/APC). After the irradiation for 1.5 h, additional 5.0 mL AA (1.0 mol/L, pH = 5.0) was added to the system, the reactor was degassed under vacuum. Then the system was irradiated under Xe lamp and repeated several times.

9. Photoelectrochemical measurements: all experiments were performed on an electrochemical workstation (Germany, Zahner Company) in a conventional three-electrode system. The resultant electrode served as the working electrode, platinum as the counter electrode and Ag/AgCl (3.0 M KCl) electrode as the reference electrode. A 20 W blue LED (λ = 450 nm) was used as the light source. A 0.5 M Na_2SO_4 aqueous solution was used as the electrolyte. The working electrodes were prepared by adding 8 μL Nafion (5%) aqueous solution into a 1 mL CdS/Cu_3N solution. Then 3.0 μL obtained solution was dropped onto a clean glassy carbon electrode with an active area of about 0.07 cm^2, which was cleaned before experiments by ultrasonication with distilled water, ethanol and isopropanol for 15 s, and dried in a vacuum.

10. DFT calculations

Details: the first principles calculations were carried out by the Materials Studio package.[6] The ion-core interaction was modeled by ultrasoft pseudopotentials[7] and the exchange–correlation (XC) functionals were described by the generalized gradient approximation (GGA) PW91 functional.[8] A 600 eV of cutoff energy was used throughout our calculations. The convergence thresholds between optimization cycles for energy change and maximum force were set as 5.0×10^{-6} eV/atom and 0.03 eV/Å, respectively. For bulk band structure calculations, an ultrafine smearing value of 0.001 Å-1 was selected to obtain accurate band gap and dispersion, where the Cu_3N (Pm-3m), Cu_3P (P-3c1), Cu_2O (Pn-3m) and Cu_2S (P63mmc) crystal structure were utilized.

In Gibbs energy ΔG calculations, a vacuum thickness of 13 Å was added to avoid the interaction of adjacent layers. In all calculations, the atoms in the bottom layers were fixed, but the atoms in the three topmost layers, as well as H atoms, were allowed to be relaxed. The dense Monkhorst-Pack grids[9] of 4×4×1 k-points were applied for the Cu_3N (100), Cu_3P (100), Cu_2O (100) and Cu_2S (001) surface. The DOS projected onto the d-states that interact with the adsorbate state can be characterized by the moments nd (ε) of the d DOS. The ε is the energy scale. The d-band center of four catalysts was calculated by formula (1):[10]

$$\varepsilon_d = \frac{\int_{-\infty}^{+\infty} n_d(\varepsilon)\varepsilon d\varepsilon}{\int_{-\infty}^{+\infty} n_d(\varepsilon) d\varepsilon} \quad (1)$$

The adsorption energy and Gibbs energy ΔG were defined in formula (2) and (3), respectively.

$$\Delta G = E_{ads} + \Delta ZPE - T\Delta S \quad (2)$$

in which $\Delta ZPE - T\Delta S$ can be assumed to be 0.24 eV[11] for H atom and

$$E_{ads} = E_{(H+slab)} - [\frac{1}{2}E_{(H_2)} + E_{(slab)}] \quad (3)$$

where the first term is the total energy of the slab with the adsorbed H^+ on the surface, the second term is the total energy of isolated H_2 molecule, and the third term is the total energy of the bare slab of the surface. According to the above definitions, a negative E_{ads} value corresponds to an exothermic adsorption, and the more negative the E_{ads}, the stronger the adsorption.

11. The calculated band structure of Cu_3N

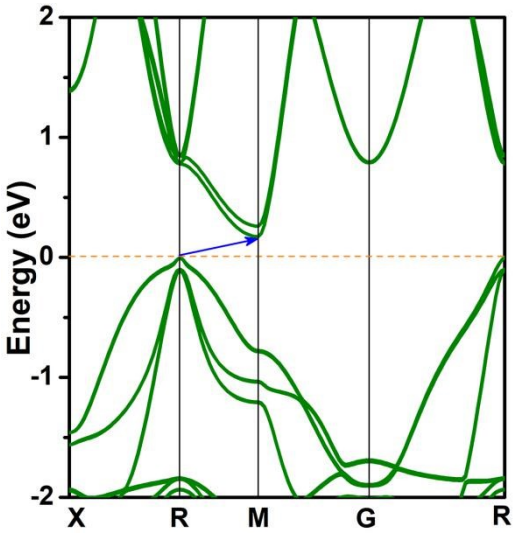

Fig. S1 The calculated band structure of Cu_3N.

12. The calculated PDOS of Cu_3N

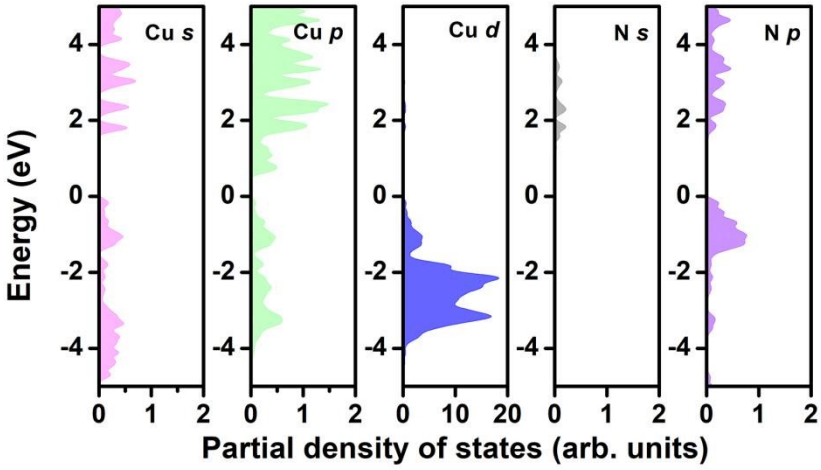

Fig. S2 The partial density of states (PDOS) of Cu_3N.

13. Crystal structure of obtained Cu_3N

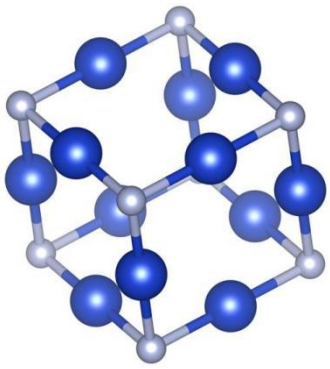

Fig. S3 The corresponding crystal structure of synthesized Cu_3N nanocrystals, showing perovskite-type P*m3m* structure. Blue and gray balls denote Cu and N atoms, respectively.

14. Full XPS spectrum of Cu_3N

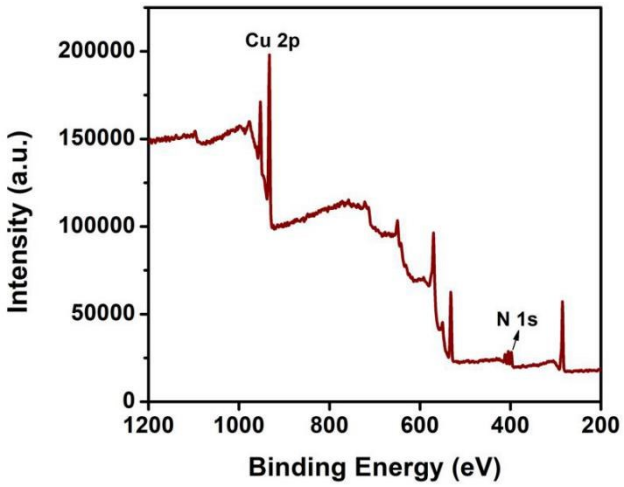

Fig. S4 Full XPS spectrum of obtained Cu_3N, indicating that both of Cu and N elements are found in the spectrum.

15. TEM images of CdS and CdS/Cu_3N

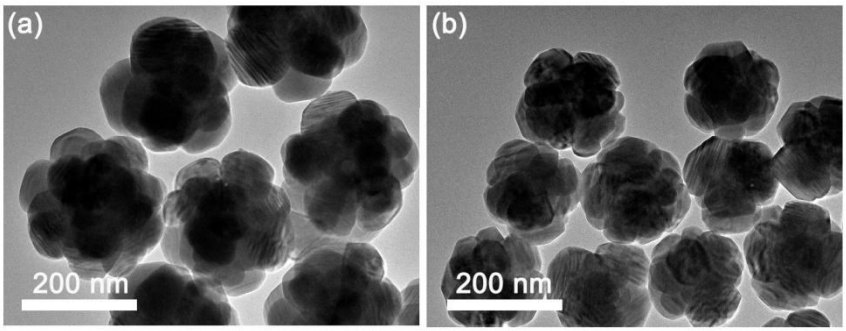

Fig. S5 TEM images of (a) CdS and (b) CdS/Cu_3N. As shown in Fig. S5, the flower-like morphology of CdS/Cu_3N is similar to that of CdS. However, the rough surface of CdS/Cu_3N was observed, indicating the integration of Cu_3N with CdS.

16. XRD patterns of various CdS/xCu_3N with different mass ratios

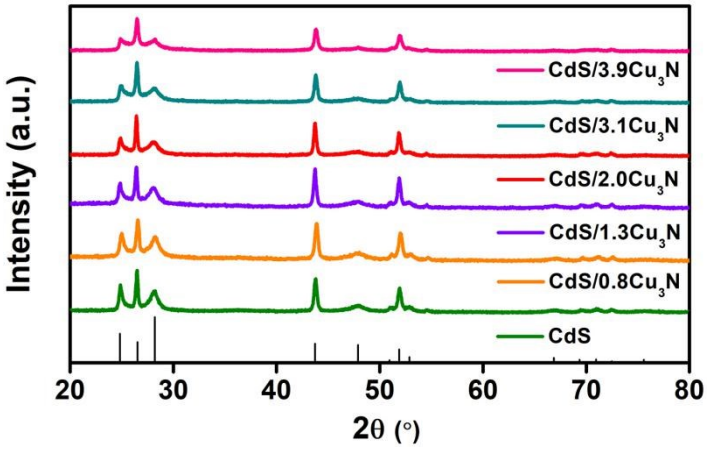

Fig. S6 XRD patterns of CdS/xCu_3N, where x denoting the mass ratio (wt.%) of Cu_3N to CdS. As shown in Fig. S6, the diffraction peaks show little change with the introduction of Cu_3N, due to the low loading and high dispersion of Cu_3N.

17. The corresponding lattice distances of CdS/Cu_3N.

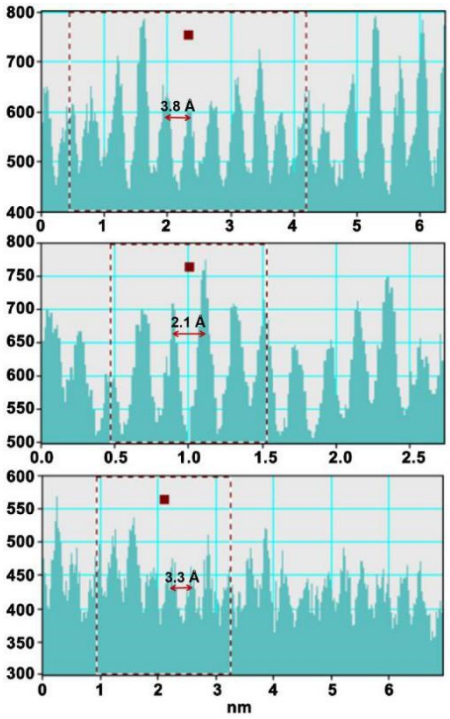

Fig. S7 The corresponding lattice distances of the exposed (100) and (111) planes of Cu_3N, and (002) plane of CdS in CdS/Cu_3N, respectively, in Fig. 2c.

18. EDX spectrum of CdS/Cu_3N

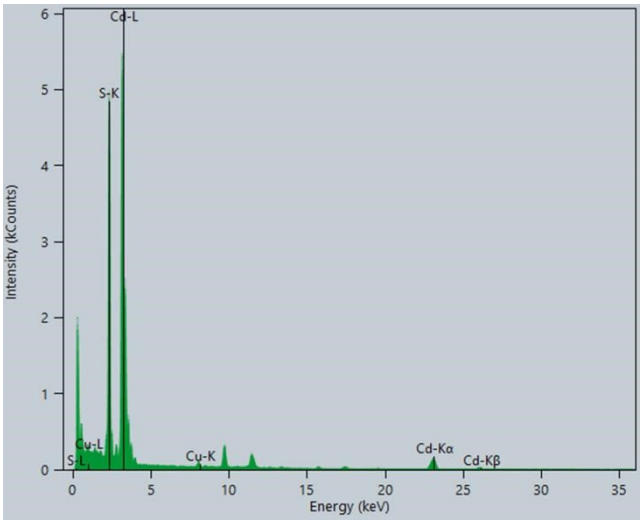

Fig. S8 EDX spectrum of obtained CdS/Cu_3N. As shown in Fig. S8, the EDX spectrum of prepared CdS/Cu_3N indicates the coexistence of elements Cd, S and Cu, implying the successful coupling of Cu_3N with CdS.

19. XPS spectrum of CdS/Cu_3N

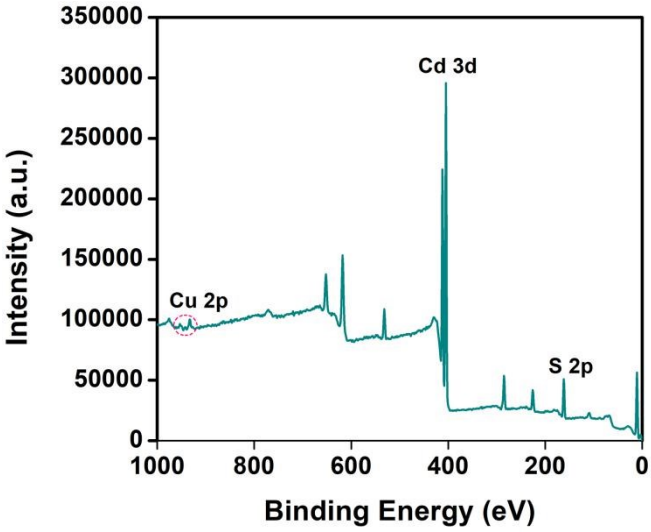

Fig. S9 Full XPS spectrum of the obtained CdS/Cu_3N, indicating that Cd, S and Cu elements are found in the spectrum.

20. High-resolution XPS spectra of Cu 2p in CdS/Cu_3N

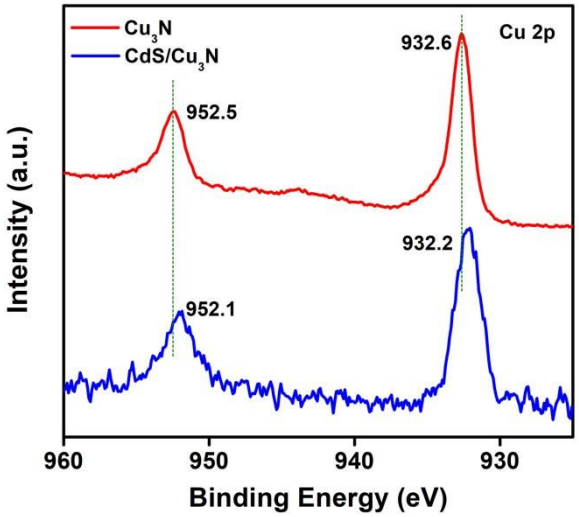

Fig. S10 High-resolution XPS spectra of Cu 2p for CdS/Cu_3N and Cu_3N. As shown in Fig. S10, the peaks of Cu (I) in Cu_3N are red shifted to ~932.2 and ~952.1 eV after integrated with CdS, further confirming the interaction of Cu_3N with CdS.[12]

21. Table. S1 Mass ratios of Cu_3N to CdS determined by ICP-AES

Samples	Dosage of Cu_3N (mg)	Cu_3N (wt.%)
CdS	0	0
CdS/0.8Cu_3N	1.0	0.8
CdS/1.3Cu_3N	2.0	1.3
CdS/2.0Cu_3N	3.0	2.0
CdS/3.1Cu_3N	5.0	3.1
CdS/3.9Cu_3N	9.0	3.9

22. UV-vis spectra of various CdS/xCu_3N with different mass ratios

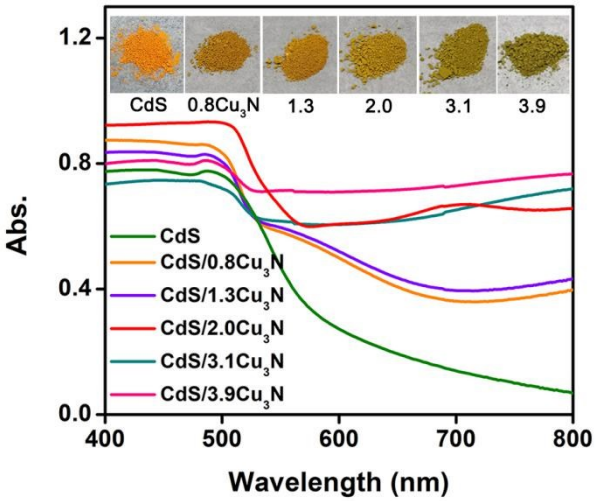

Fig. S11 UV-vis spectra of CdS/xCu_3N (x denoting the mass ratio (wt.%) of Cu_3N to CdS) samples with different dosages of Cu_3N. The inset shows the colors of the above samples.

23. Table. S2 Comparison of photocatalytic activity with reported CdS-based system

Photocatalysts	Electron donor	Light source	H_2 generation rate (mmol $g^{-1}h^{-1}$)	Enhancem-ent factor	AQY (%)	Reference
CdS/C60/TiO_2	0.25 M Na_2S, 0.35 M Na_2SO_3	350 W Xe lamp	0.12	8.5	2.0 (420 nm)	*ACS Appl. Mater. Interfaces* **2015**, *7*, 4533.
CdS/Sn^{2+}	glycerol	350 W Xe lamp	1.61	24	10.9 (420 nm)	*Small* **2020**, *16*, 2001024.
CdS/NiS	lactic acid	300 W Xe lamp	158.7	250	74.1 (420 nm)	*Chem. Sci.*, **2018**, *9*, 1574.
CdS/MoS_2	lactic-acid	300 W Xe lamp	6.02	28	22.0 (475 nm)	*Nano Res.* **2017**, *10*, 1377.
CdS/Mo_2N	1.0 M Na_2S, 1.0 M Na_2SO_3	300 W Xe lamp	0.97	6.1	2.2 (420 nm)	*Int. J. Hydrogen Energy* **2016**, *41*, 22009.
CdS/Ni	methanol	300 W Xe lamp	3.74	133	2.2 (400 nm)	*Int. J. Hydrogen Energy* **2015**, *40*, 998.
CdS/Pt	lactic acid	300 W Xe lamp	16.27	7.7	N/A	*J. Mater. Chem. A*, **2015**, *3*, 23732.
CdS/CuS	0.25 M Na_2S, 0.35 M Na_2SO_3	500 W Xe lamp	0.33	3.5	N/A	*Int. J. Hydrogen Energy* **2013**, *38*, 11811.
CdS/Cu_3N	**ascorbic acid**	**300 W Xe lamp**	**4.5**	**851**	**3.9 (450 nm)**	**this work**

24. Wavelength-dependent activity of CdS/Cu_3N for H_2 production

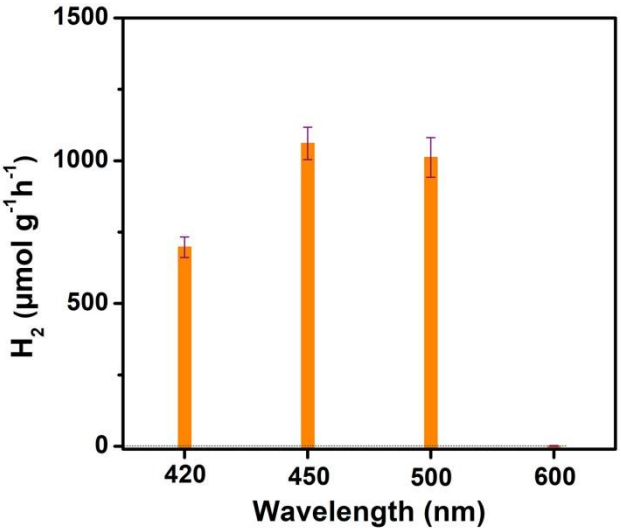

Fig. S12 Wavelength-dependent activity of CdS/Cu_3N for H_2 generation.

25. Stability of CdS/Cu_3N for H_2 production

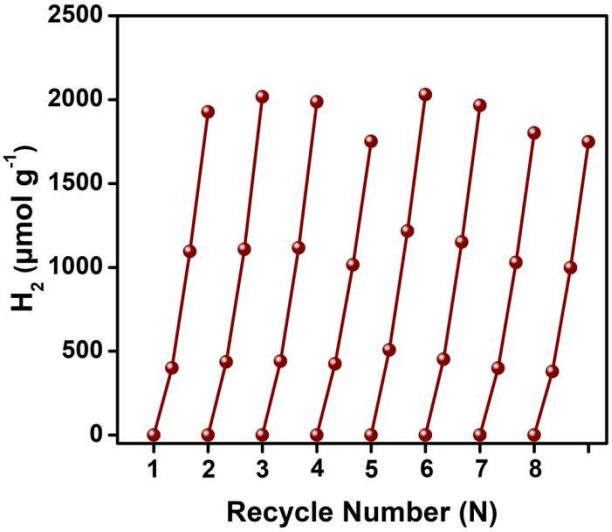

Fig. S13 Stability of photocatalytic H_2 evolution reaction using CdS/Cu_3N as a photocatalyst and ascorbic acid as a sacrificial reagent. As shown in Fig. S13, even after 8 recycles of the photocatalytic reaction, the system remains 91% of the initial H_2 evolution activity, signifying an excellent stability.

26. XRD pattern of recycled CdS/Cu_3N

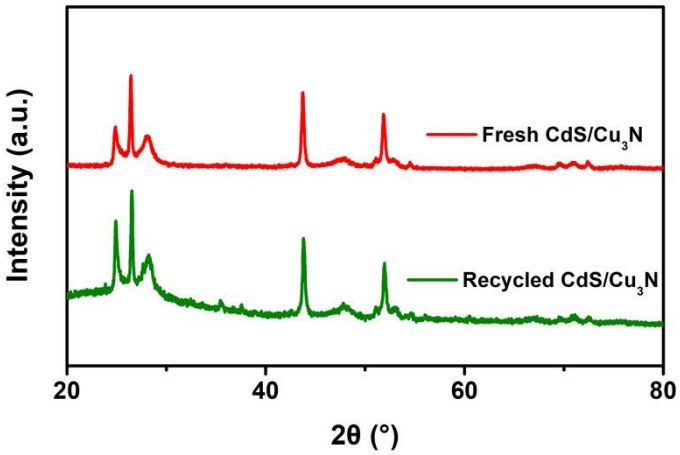

Fig. S14 XRD pattern of fresh and recycled CdS/Cu_3N after 8 cycle tests.

27. Elemental mapping of recycled CdS/Cu_3N

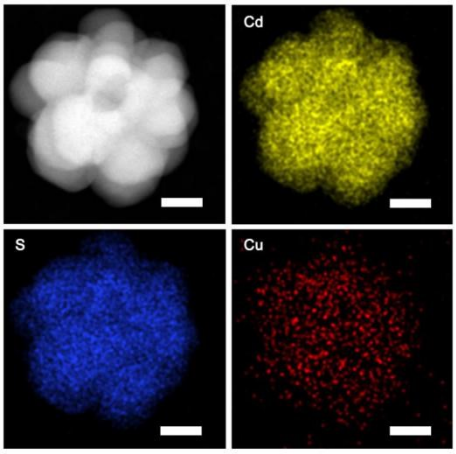

Fig. S15 TEM image of recycled CdS/Cu_3N architecture and corresponding elemental mapping of Cd, S and Cu, respectively.

28. XRD patterns of Cu_2O, Cu_2S and Cu_3P

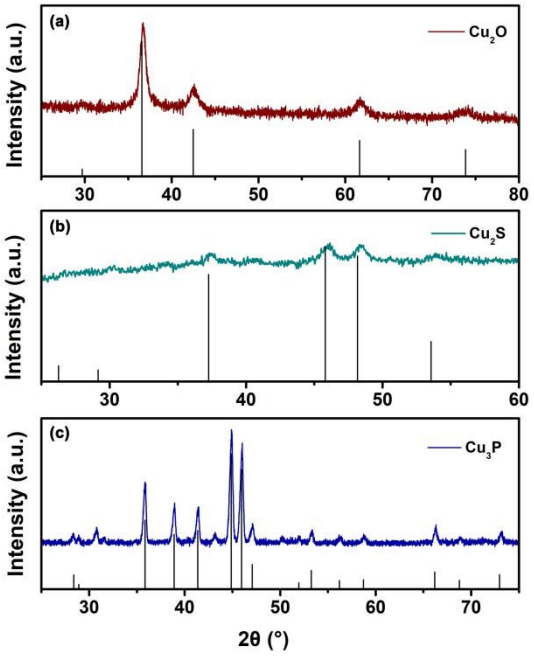

Fig. S16 XRD patterns of the prepared (a) Cu_2O, (b) Cu_2S and (c) Cu_3P, which match well with the standard Cu_2O (PDF No. 74-1230), Cu_2S (PDF No. 84-0206) and Cu_3P (PDF No. 74-1067), respectively.[3-5]

29. Activity comparison of Cu_3N with other Cu(I)-based cocatalysts

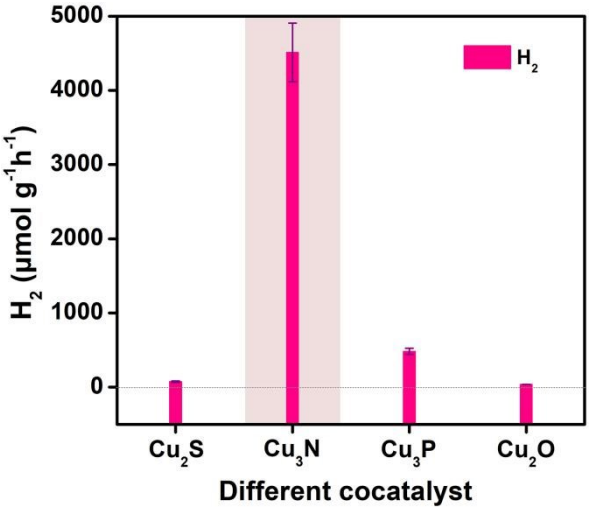

Fig. S17 Comparison of photocatalytic H_2 generation activity of CdS/Cu_3N with that of CdS/Cu_2S, CdS/Cu_3P, CdS/Cu_2O under identical conditions.

30. UV-vis diffuse reflectance spectra and corresponding *Tauc* Plots of CdS/Cu_3N

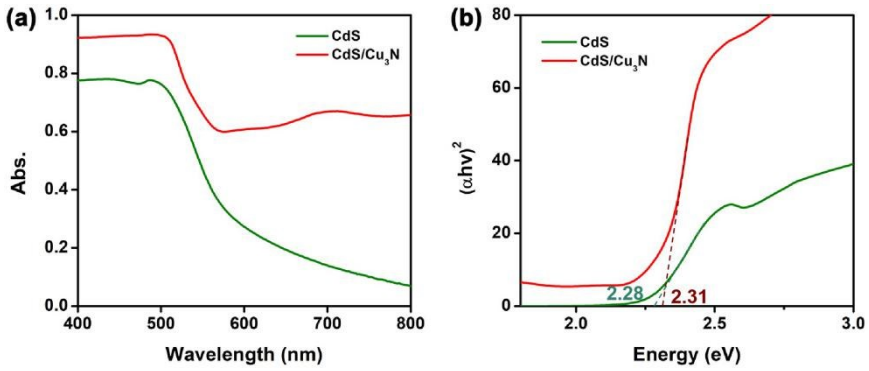

Fig. S18 (a) UV-vis diffuse reflectance spectra and (b) corresponding *Tauc* plots of obtained CdS and CdS/Cu_3N. As shown in Fig. S18a, CdS/Cu_3N exhibits a stronger visible-light absorption and a red-shifted absorption edge compared to CdS, indicating more powerful visible-light harvesting. In addition, CdS/Cu_3N shows a band gap of ~2.31 eV from the corresponding *Tauc* plot (Fig. S18b).

31. Mott-Schottky plots of CdS/Cu_3N

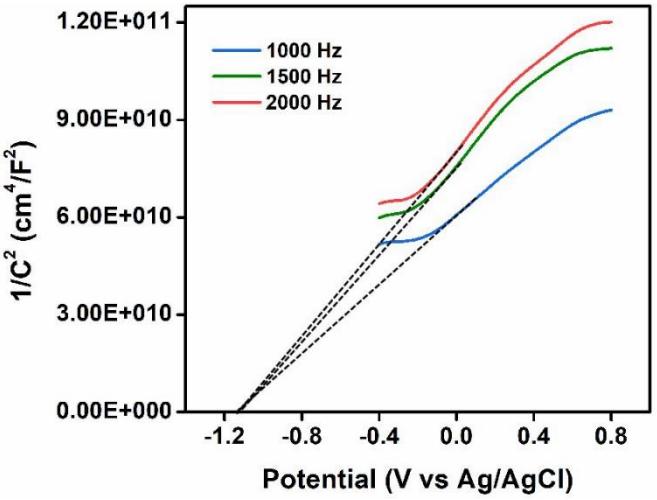

Fig. S19 Mott-Schottky plots of CdS/Cu_3N at frequencies of 1000, 1500 and 2000 Hz. As shown in Fig. S19, flat band potential of CdS/Cu_3N can be estimated as -1.1 V *vs* Ag/AgCl.[13]

32. Band structure diagram of CdS/Cu_3N

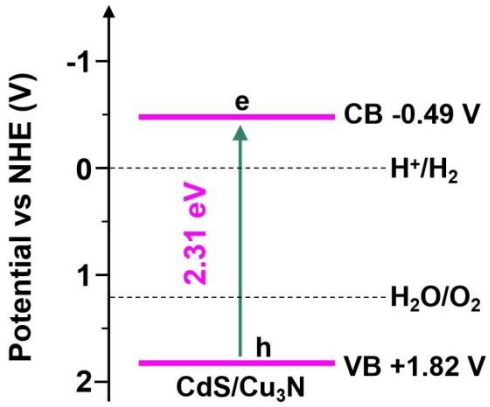

Fig. S20 Schematic illustration for the band structure of CdS/Cu_3N. As shown in Fig. S20, it is thermodynamically feasible for the proton reduction reaction on CdS/Cu_3N.

33. Table. S3 Fitted parameter of PL lifetime in Fig. 4b

Sample	B_1	B_2	τ_1 / ns	τ_2 / ns	τ / ns
CdS	6.98E-02	8.68E-03	1.44	5.285	2.6
CdS/Cu_3N	5.49E-02	1.51E-02	1.64	6.89	4.5

The emission decay of CdS in the absence and presence of Cu_3N were studied and the decay curves for the samples were well fitted with double-exponential function *Y*(t) based on nonlinear least-squares, using the following equation:

$$Y(t) = B_1 \exp(-t / \tau_1) + B_2 \exp(-t / \tau_2)$$

Where B_1, B_2 are fractional contributions from time-resolved emission decay lifetime τ_1, τ_2, as shown in Table S2. The average lifetime τ could be obtained from the following equation:

$$< \tau >= \frac{B_1 {\tau_1}^2 + B_2 {\tau_2}^2}{B_1 \tau_1 + B_2 \tau_2}$$

34. References

1. a) D. D. Vaughn II, J. Araujo, P. Meduri, J. F. Callejas, M. A. Hickner and R. E. Schaak, *Chem. Mater*. 2014, **26**, 6226; b) H. Wu and W. Chen, *J. Am. Chem. Soc.* 2011, **133**, 15236.

2. D. Wang, Y. Li, *Chem. Commun.* 2011, **47**, 3604.

3. Z. Zhuang, Q. Peng, B. Zhang and Y. Li, *J. Am. Chem. Soc*. 2008, **130**, 10482.

4. R. Shen, J. Xie, X. Lu, X. Chen and X. Li, *ACS Sustainable Chem. Eng.* 2018, **6**, 4026.

5. J. Ran, G. Gao, F. T. Li, T. Y. Ma, A. Du and S. Z. Qiao, *Nat Commun* 2017, **8**, 13907.

6. S. Clark, M. Segall, C. Pickard, P. Hasnip, M. Probert, K. Refson and M. Payne, *Z Kristallogr* 2005, **220***,* 567.

7. D. Vanderbilt, *Phys Rev B* 1990, **41**, 7892.

8. J. P. Perdew, K. Burke and M. Ernzerhof, *Phys Rev Lett* 1996, **77**, 3865.

9. H. J. Monkhorst, J. D. Pack, *Phys Rev B* 1976, **13**, 5188.

10. J. K. Nørskov, F. Studt, F. Abild-Pedersen and T. Bligaard, *John Wiley & Sons, Inc*., 2014. **1114**.

11. B. Hinnemann, P. G. Moses, J. Bonde, K. P. Joergensen, J. H. Nielsen, S. Horch, I. Chorkendorff and J. K. Noerskov, *J. Am. Chem. Soc.* 2005, **127**, 5308-5309

12. Z. Wang, L. Xu, F. Huang, L. Qu, J. Li, K. A. Owusu, Z. Liu, Z. Lin, B. Xiang, X. Liu, K. Zhao, X. Liao, W. Yang, Y. B. Cheng and L. Mai, *Adv Engery Mater* 2019, **9***,* 1900390.

13. G. Wang, T. Zhang, W. Yu, R. Si, Y. Liu and Z. Zhao, *ACS Catal.* 2020**, 10,** 5715.